Nonlinear buckling analysis of clamped-free porous FG cylindrical sandwich shells

Mohsen Rahmani[1,*]
[1] Department of Mechanics, Tuyserkan Branch, Islamic Azad University, Tuyserkan, Iran

ABSTRACT

Based on a modified higher order sandwich shell theory, the buckling behaviors of cylindrical sandwich shells are investigated. Sandwiches consist of two functionally graded face-sheets and a homogenous core. Functionally graded materials are varied gradually across the thickness based on a power law rule which modified by considering the even and uneven porosity distributions. All materials are temperature dependent. Nonlinear Von-Karman strain, thermal stresses in all layers and in-plane strain and transverse flexibility of the core are considered to obtain the governing equations based on the minimum potential energy principle. A Galerkin method is used to solve in clamped-free boundary condition under an axial in-plane compressive load. The results of the present method are compared with some literatures to verify the procedure. Also, the effect of variation of temperature, some geometrical parameters and porosities on the critical load are studied.

Keywords: Porosity, Temperature-dependent, FGM, Buckling, Clamped-free, Sandwich shell

1. INTRODUCTION

High performance and high bending rigidity with a low weight make the modern industries such as nuclear reactor, aerospace, marine, satellite, aircraft, sport devices and construction to use the sandwich structures which usually composed of two thin and stiff face sheets that cover a thick and soft core. To avoid the delamination, stress concentration and failure in the ordinary composite materials and laminates in the sandwich panels in high temperature conditions, functionally graded materials have been proposed by Japanese scientists which are in-homogeneous microscopic materials and their properties vary across the thickness smoothly. But during the manufacturing the FGMs, some micro voids are appeared that affect the materials properties, so the porosity distributions should be considered to modify the models of FGMs. Also, the high temperature conditions affect the material properties, so it is important to consider the dependency of materials properties to the temperature [1, 2].

In the classical plate and shell theories, the core is considered as an inflexible layer, but to accurate investigation of the mechanical behavior of sandwich structures and detect some local modes, the core should be considered as a transversely flexible layer. So, the high order sandwich theory was presented [3]. Many researchers have been studied the mechanical behaviors of cylindrical sandwich shells such as buckling and post-buckling by using different theories. Lopatin and Morozov presented the buckling analysis of fully clamped composite sandwich cylindrical shell subjected to uniform lateral pressure by using the Galerkin method [4]. Shahgholian and Rahimi investigated the global buckling of composite cylindrical shells with lattice cores under uniaxial compression based on the smeared stiffener method and using Rayleigh-Ritz method [5]. Hieu et al. studied the buckling and postbuckling behavior of FGM sandwich cylindrical shells subjected to external pressure in thermal conditions based on the classical shell theory and using Galerkin method [6]. Daikh studied the thermal buckling of FG sandwich cylindrical shell based on the Donnell theory. Material properties was modelled by sigmoid function and the thermal uniform, linear and nonlinear loads distributions were considered [7].Based on the Donnell shell theory and smeared technique, Nam et al. studied the nonlinear torsional buckling and postbuckling of sandwich FG cylindrical shells reinforced by stiffeners under thermal conditions [8]. Fallah and Taati studied the nonlinear bending and post-buckling of laminated sandwich cylindrical shells with isotropic, FG or isogrid core under the thermo-mechanical loadings and different boundary conditions [9]. Balbin and Bisagni studied the buckling of sandwich

cylindrical shells with composite face sheets and a deformable core [10]. Based on the Donnell shell theory, Chan et al. studied the nonlinear buckling and postbuckling of imperfect FG porous sandwich cylindrical panels subjected to axial loading under various boundary conditions [11]. Hung et al. studied the nonlinear buckling and post buckling of spiral corrugated sandwich FG cylindrical shells under external pressure resting on the elastic foundation and based on the Donnell shell theory and using a Galerkin method to solve the problems [12]. Semenyuk et al. investigated the stability and initial post-buckling behavior of orthotropic cylindrical sandwich shells by asymptotic Koiter–Budiansky method [13]. Malekzadeh et al. studied the free vibration and buckling analysis of cylindrical sandwich panel with magneto rheological layer based on an improved higher order sandwich panel theory [14]. Shatov et al. studied the buckling of sandwich cylindrical shell with composite lattice core under hydrostatic pressure based on a finite element method [15]. Nam et al. investigated the nonlinear buckling and post-buckling of FG porous circular cylindrical shells reinforced by orthogonal stiffeners resting on elastic foundation in thermal condition and under torsional load by using the classical shell theory [16]. Phuong et al. investigated the nonlinear stability of FG sandwich cylindrical shells with stiffeners under axial compression in thermal conditions based on the Donnell shell theory [17]. Han et al. studied the buckling behavior of cylinder shell with FGM coating under the thermal condition [18]. Evkin presented mathematical model of local buckling of cylindrical shells based on Pogorelov's geometrical method [19]. Trablesi et al. studied the thermal buckling of FG plates and cylindrical shells by usisng a modified first order shear deformation theory [20]. Mehralian and Beni studied the size-dependent torsional buckling behavior of FG cylindrical shell based on modified couple stress theory using shell model and GDQ method [21]. Fan studied the critical buckling load of compresses cylindrical shell based on the non-destructive probing method [22]. Sofiyev and Hui studied the vibration and stability of FG cylindrical shells under the external pressure based on the first order shear deformation theory and Galerkin method [23]. Based on the Donnell shell theory, Gao et al. studied the dynamic stability behavior of FG orthotropic cylindrical shell resting on the elastic foundation [24]. Sheng and Wang studied the dynamic stability and nonlinear vibration of stiffened FG cylindrical shell in thermal condition by using FSDT, smearing method and Bolotin method [25]. Sofiyev et al. studied the effect of shear stresses and rotary inertia on the stability and vibration of sandwich cylindrical shells with FG core resting on the elastic medium based on the FSDT [26]. Asai et al. investigated the thermal instability of geometrically imperfect sandwich cylindrical shells under uniform heating based on the Brinson phenomenological model and third order shear deformation theory. The sandwich were made of FG face sheets and a SMA fiber reinforced composite core [27].

By reviewing the accessible references, it's found that more investigation should be done in the critical load responses. To study the buckling behavior of FG sandwich cylindrical shells in the uniform temperature distributions under the clamped-free boundary condition, a modified high order sandwich shell theory is used to detect the more accurate modes. Sandwich consists of a homogeneous core which covered by FG face sheets. A power law rule which modified by considering the even and uneven porosity distributions are used to model the gradually variation of the FGMs. Also, all materials are considered temperature dependent. In-plane stresses and high order stresses of the core, and thermal stresses and thermal stress resultants of the face-sheets and core, which usually ignored by the researchers, are considered in this paper. The equations are derived based on the minimum potential energy principle under an axial compression and nonlinear Von-Karman strains are used. A Galerkin method is used to solve the equations. The effects of the temperature variation, some geometrical parameters and porosity variation on the critical load of sandwich cylindrical shell are investigated, too.

2. FORMULATION

Consider a FG sandwich cylindrical shell with a homogeneous core which covered by two porous FG face sheets, as shown in Fig.1.

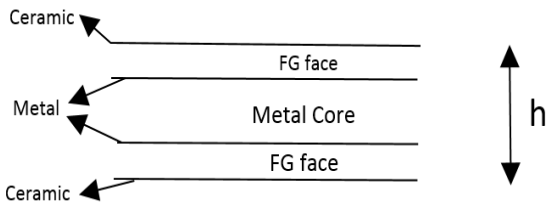

Fig. 1. Schematic of sandwich cylindrical shell

All materials are temperature dependent which modelled as follows [28]:

$$P = P_0\left(P_{-1}T^{-1} + 1 + P_1T + P_2T^2 + P_3T^3\right) \quad (1)$$

where "P"s are coefficients of temperature, and they are unique for each material; T=T0+ΔT, which T0 is equal to 300(K). A power law rule which consists of even porosity volume fraction is presented to model the FGM properties as follow [28]:

$$P_j\left(z_j,T\right) = g\left(z_j\right)P_{ce}^{j}\left(T\right) + \left[1-g\left(z_j\right)\right]P_m^j\left(T\right) - \left(P_{ce}^{j}\left(T\right) + P_m^j\left(T\right)\right)\frac{\zeta}{2};\quad j=(o,i) \quad (2)$$

$$g\left(z_o\right) = \left(\frac{\frac{h_o}{2}-z_o}{h_o}\right)^N;\quad g\left(z_i\right) = \left(\frac{\frac{h_i}{2}+z_i}{h_i}\right)^N; \quad (3)$$

where "N" is the constant power law index; g(z) and [1-g(z)] are volume fraction of ceramic and metal; "ζ" is the porosity distribution; and subscripts "o", "i" and "c" refer to outer and inner faces and the core, respectively. In the uneven case, the micro voids are spread in the middle area of the layers and decrease near to the edges and tend to the zero. So, power law rule in the uneven case is modified as follows [28]:

$$P_j\left(z_j,T\right) = g\left(z_j\right)P_{ce}^{j}\left(T\right) + \left[1-g\left(z_j\right)\right]P_m^j\left(T\right) - \left(P_{ce}^{j}\left(T\right) + P_m^j\left(T\right)\right)\frac{\zeta}{2}\left(1-\frac{2|z|}{h}\right) \quad (4)$$

The minimum potential energy principle is used to obtain the governing equations of sandwich cylindrical shells which include potential of the external loads, "V", and total strain energy, "U"; This principle is presented as follows [29]:

$$\prod\left(\delta U + \delta V\right) = 0 \quad (5)$$

which "δ" denotes the variation operator. The variation of the total strain energy includes mechanical stresses and thermal stresses with nonlinear strains in the faces and core. The compatibility conditions rule as constraints which are attended as six Lagrange multipliers in the principle. By considering the in-plane stresses of the core, "δU" is as follows:

$$\begin{aligned}
\delta U =& \int_{V_o}(\sigma_{ss}^{o}\delta\varepsilon_{ss}^{o} + \sigma_{s}^{oT}\delta d_{ss}^{o} + \sigma_{\theta\theta}^{o}\delta\varepsilon_{\theta\theta}^{o} + \sigma_{\theta\theta}^{oT}\delta d_{\theta\theta}^{o} + \tau_{s\theta}^{o}\delta\gamma_{s\theta}^{o} + \tau_{sz}^{o}\delta\gamma_{sz}^{o} + \tau_{\theta z}^{o}\delta\gamma_{\theta z}^{o})dV_o \\
&+\int_{V_i}(\sigma_{ss}^{i}\delta\varepsilon_{ss}^{i} + \sigma_{s}^{iT}\delta d_{ss}^{i} + \sigma_{\theta\theta}^{i}\delta\varepsilon_{\theta\theta}^{i} + \sigma_{\theta\theta}^{iT}\delta d_{\theta\theta}^{i} + \tau_{s\theta}^{i}\delta\gamma_{s\theta}^{i} + \tau_{sz}^{i}\delta\gamma_{sz}^{i} + \tau_{\theta z}^{i}\delta\gamma_{\theta z}^{i})dV_i \\
&+\int_{V_c}(\sigma_{ss}^{c}\delta\varepsilon_{ss}^{c} + \sigma_{s}^{iT}\delta d_{ss}^{i} + \sigma_{\theta\theta}^{c}\delta\varepsilon_{\theta\theta}^{c} + \sigma_{\theta\theta}^{cT}\delta d_{\theta\theta}^{c} + \sigma_{zz}^{c}\delta\varepsilon_{zz}^{c} + \sigma_{zz}^{cT}\delta d_{zz}^{c} + \tau_{s\theta}^{c}\delta\gamma_{s\theta}^{c} + \tau_{sz}^{c}\delta\gamma_{sz}^{c} + \tau_{\theta z}^{c}\delta\gamma_{\theta z}^{c})dV_c \\
&+\delta\int_0^{L}\int_0^{2\pi}[\lambda_{so}\left(u_o\left(z_o=h_o/2\right)-u_c\left(z_c=-h_c/2\right)\right) + \lambda_{\theta o}\left(v_o\left(z_o=h_o/2\right)-v_c\left(z_c=-h_c/2\right)\right) \\
&+\lambda_{zo}\left(w_o\left(z_o=h_o/2\right)-w_c\left(z_c=-h_c/2\right)\right) + \lambda_{si}\left(u_c\left(z_c=h_c/2\right)-u_i\left(z_i=-h_i/2\right)\right) \\
&+\lambda_{\theta i}\left(v_c\left(z_c=h_c/2\right)-v_i\left(z_i=-h_i/2\right)\right) + \lambda_{zi}\left(w_c\left(z_c=h_c/2\right)-w_i\right)]rdsd\theta
\end{aligned} \quad (6)$$

where σss, σθθ and τsθ display the in-plane normal and shear stresses; εss, εθθ and γsθ are the in plane normal and shear strains of the layers; σTss and σTθθ express the thermal stresses; σczz and εczz present the lateral normal stress and strain in the core; τcsz, τcθz, γcsz and γcθz declare shear stresses and shear strains in the core; and λs, λθ and λz are the Lagrange multipliers at the face sheet-core interfaces. It should be noted that the material properties in the functionally graded layers are the function of the displacement and the temperature, and in the homogeneous layer are just function of the temperature.

The variation of the external loads as follows [30]:

$$\delta V = -\int_0^{L}\int_0^{2\pi}(P_o\delta w_{0o} + P_i\delta w_{0i} + n_s^{o}\delta u_{0o} + n_s^{i}\delta u_{0i})r\,d\theta ds \quad (7)$$

where "u_0^j" and w_0^j(j = o, i) are the displacements of the mid-plane of the face sheets in the longitudinal and vertical directions, respectively; "n_s^j" are the in-plane external loads of the top and bottom face sheets; and, "P_o" and "P_i" are the vertical distributed loads applied on the top and bottom face sheets, respectively.

The displacement fields of the face sheets are modelled by the first order shear deformation theory.

$$u_j(s,\theta,z_j)=u_{0j}(s,\theta)+z_j\phi_s^j(s,\theta);\ j=(o,i) \quad (8)$$

$$v_j(s,\theta,z_j)=v_{0j}(s,\theta)+z_j\phi_\theta^j(s,\theta) \quad (9)$$

$$w_j(s,\theta,z_j)=w_{0j}(s,\theta) \quad (10)$$

where subscript "0" expresses values in association with the middle surface of the layers; and "ϕ" is the rotation of the normal to the middle surface. The kinematic relations of the core are presented as cubic patterns which contain eleven unknown coefficients as follows:

$$u_c(s,\theta,z_c)=u_0(s,\theta)+u_1(s,\theta)z_c+u_2(s,\theta){z_c}^2+u_3(s,\theta){z_c}^3 \quad (11)$$

$$v_c(s,\theta,z_c)=v_0(s,\theta)+v_1(s,\theta)z_c+v_2(s,\theta){z_c}^2+v_3(s,\theta){z_c}^3 \quad (12)$$

$$w_c(s,\theta,z_c)=w_0(s,\theta)+w_1(s,\theta)z_c+w_2(s,\theta){z_c}^2 \quad (13)$$

The nonlinear Von-Karman strain-displacement relations for the face sheets (j=o, i) can be defined as [1, 2]:

$$\varepsilon_{ss}^{j}=u_{0j,s}+z_j\varphi_{s,s}^{j}+\frac{1}{2}{w_{j,s}}^2-\alpha_j\Delta T_j \quad (14)$$

$$\varepsilon_{\theta\theta}^{j}=\frac{1}{r}\left(v_{0j,\theta}+z_j\varphi_{\theta,\theta}^{j}+w_j\right)+\frac{1}{2r^2}{w_{j,\theta}}^2-\alpha_j\Delta T_j \quad (15)$$

$$\varepsilon_{zz}^{j}=-\alpha_j\Delta T_j \quad (16)$$

$$\gamma_{s\theta}^{j}=\frac{1}{r}\left(u_{0j,\theta}+z_j\varphi_{s,\theta}^{j}\right)+v_{0j,s}+z_j\varphi_{\theta,s}^{j}+\frac{1}{r}w_{j,s}w_{j,\theta} \quad (17)$$

$$\gamma_{sz}^{j}=\varphi_s^j+w_{j,s} \quad (18)$$

$$\gamma_{\theta z}^{j}=\frac{1}{r}\left(w_{j,\theta}-v_{0j}-z_j\varphi_\theta^j\right)+\varphi_\theta^j \quad (19)$$

The"(),i" expresses derivation with respect to "i". The strain of the core can be defined as:

$$\varepsilon_{ss}^{c}=u_{0,s}+u_{1,s}z_c+u_{2,s}{z_c}^2+u_{3,s}{z_c}^3+\frac{1}{2}{w_{0,s}}^2-\alpha_c\Delta T_c \quad (20)$$

$$\varepsilon_{\theta\theta}^{c}=\frac{1}{r}\left[v_{0,\theta}+v_{1,\theta}z_c+v_{2,\theta}{z_c}^2+v_{3,\theta}{z_c}^3+\left(w_0+w_1z_c+w_2{z_c}^2\right)\right]+\frac{1}{2r^2}{w_{0,\theta}}^2-\alpha_c\Delta T_c \quad (21)$$

$$\varepsilon_{zz}^{c}=w_1+2w_2z_c-\alpha_c\Delta T_c \quad (22)$$

$$\gamma_{sz}^{c}=\left(u_1+2u_2z_c+3u_3{z_c}^2\right)+\left(w_{0,s}+w_{1,s}z_c+w_{2,s}{z_c}^2\right) \quad (23)$$

$$\gamma_{\theta z}^{c}=\frac{1}{r}\left[w_{0,\theta}+w_{1,\theta}z_c+w_{2,\theta}{z_c}^2-\left(v_0+v_1z_c+v_2{z_c}^2+v_3{z_c}^3\right)\right]+v_1+2v_2z_c+3v_3{z_c}^2 \quad (24)$$

$$\gamma_{s\theta}^{c}=\frac{1}{r}\left[u_{0,\theta}+u_{1,\theta}z_c+u_{2,\theta}{z_c}^2+u_{3,\theta}{z_c}^3+w_{0,s}w_{0,\theta}\right]+v_{0,s}+v_{1,s}z_c+v_{2,s}{z_c}^2+v_{3,s}{z_c}^3 \quad (25)$$

It is assumed that core is perfectly bonded to the face sheets. So, the compatibility conditions between core and face-sheets which obtained by Lagrange multipliers in Eq. (6) are as follows:

$$u_o(z_o=h_o/2)=u_c(z_c=-h_c/2) \quad (26)$$

$$v_o(z_o=h_o/2)=v_c(z_c=-h_c/2) \quad (27)$$

$$w_o=w_c(z_c=-h_c/2) \quad (28)$$

$$u_c(z_c=h_c/2)=u_i(z_i=-h_i/2) \quad (29)$$

$$v_c(z_c=h_c/2)=v_i(z_i=-h_i/2) \quad (30)$$

$$w_c\left(z_c = h_c/2\right) = w_i \tag{31}$$

Based on compatibility conditions, the displacements of the face-sheets are dependent to the core, so the unknown decrease to fifteen and the number of the governing equations are fifteen.

$$+r\frac{h_o}{2}N^{\,o}_{ss,s} - rM^{\,o}_{ss,s} + \frac{h_o}{2}N^{\,o}_{s\theta,\theta} - M^{\,o}_{s\theta,\theta} + rN^{\,o}_{sz} - \frac{h_o}{2}n^o_s = 0 \tag{32}$$

$$+\frac{h_o}{2}N^{\,o}_{\theta\theta,\theta} - M^{\,o}_{\theta\theta,\theta} + \frac{h_o}{2}rN^{\,o}_{s\theta,s} - rM^{\,o}_{s\theta,s} - M^{\,o}_{\theta z} + rN^{\,o}_{\theta z} + \frac{h_o}{2}N^{\,o}_{\theta z} - \frac{h_o}{2}n^o_s = 0 \tag{33}$$

$$-r\frac{h_i}{2}N^{\,i}_{ss,s} - rM^{\,i}_{ss,s} - \frac{h_i}{2}N^{\,i}_{s\theta,\theta} - M^{\,i}_{s\theta,\theta} + rN^{\,i}_{sz} + \frac{h_i}{2}n^i_s = 0 \tag{34}$$

$$-\frac{h_i}{2}N^{\,i}_{\theta\theta,\theta} - M^{\,i}_{\theta\theta,\theta} - \frac{h_i}{2}rN^{\,i}_{s\theta,s} - rM^{\,i}_{s\theta,s} - M^{\,i}_{\theta z} + rN^{\,i}_{\theta z} - \frac{h_i}{2}N^{\,i}_{\theta z} + \frac{h_i}{2}n^i_s = 0 \tag{35}$$

$$-rN^{\,o}_{ss,s} - N^{\,o}_{s\theta,\theta} - rN^{\,i}_{ss,s} - N^{\,i}_{s\theta,\theta} - rR^{c}_{ss,s} - Q^{c}_{s\theta,\theta} + n^o_s + n^i_s = 0 \tag{36}$$

$$+r\frac{h_c}{2}N^{\,o}_{ss,s} - r\frac{h_c}{2}N^{\,i}_{ss,s} + \frac{h_c}{2}N^{\,o}_{s\theta,\theta} - \frac{h_c}{2}N^{\,i}_{s\theta,\theta} - rM^{\,i}_{s1,s} - M^{c}_{Q1s\theta,\theta} + rQ^{c}_{sz} + \frac{h_c}{2}n^o_s + \frac{h_c}{2}n^i_s = 0 \tag{37}$$

$$-r\frac{h_c^2}{4}N^{\,o}_{ss,s} - r\frac{h_c^2}{4}N^{\,i}_{ss,s} - \frac{h_c^2}{4}N^{\,o}_{s\theta,\theta} - \frac{h_c^2}{4}N^{\,i}_{s\theta,\theta} - rM^{\,i}_{s2,s} - M^{c}_{Q2s\theta,\theta} + 2rM^{c}_{Q1sz} + \frac{h_c^2}{4}n^o_s + \frac{h_c^2}{4}n^i_s = 0 \tag{38}$$

$$+r\frac{h_c^3}{8}N^{\,o}_{ss,s} - r\frac{h_c^3}{8}N^{\,i}_{ss,s} + \frac{h_c^3}{8}N^{\,o}_{s\theta,\theta} - \frac{h_c^3}{8}N^{\,i}_{s\theta,\theta} - rM^{\,i}_{s3,s} - M^{c}_{Q3s\theta,\theta} + 3rM^{c}_{Q2sz} - \frac{h_c^3}{8}n^o_s + \frac{h_c^3}{8}n^i_s = 0 \tag{39}$$

$$-N^{\,o}_{\theta\theta,\theta} - N^{\,i}_{\theta\theta,\theta} - rN^{\,o}_{s\theta,s} - rN^{\,i}_{s\theta,s} - N^{\,o}_{\theta z} - N^{\,i}_{\theta z} - R^{c}_{\theta,\theta} - rQ^{c}_{s\theta,s} - Q^{c}_{\theta z} + n^o_s + n^i_s = 0 \tag{40}$$

$$+\frac{h_c}{2}N^{\,o}_{\theta\theta,\theta} - \frac{h_c}{2}N^{\,i}_{\theta\theta,\theta} + r\frac{h_c}{2}N^{\,o}_{s\theta,s} - r\frac{h_c}{2}N^{\,i}_{s\theta,s} + \frac{h_c}{2}N^{\,o}_{\theta z} - \frac{h_c}{2}N^{\,i}_{\theta z} - M^{c}_{\theta1,\theta} - rM^{c}_{Q1s\theta,s} - M^{c}_{Q10z}$$
$$+rQ^{c}_{\theta z} - \frac{h_c}{2}n^o_s + \frac{h_c}{2}n^i_s = 0 \tag{41}$$

$$-\frac{h_c^2}{4}N^{\,o}_{\theta\theta,\theta} - \frac{h_c^2}{4}N^{\,i}_{\theta\theta,\theta} - r\frac{h_c^2}{4}N^{\,o}_{s\theta,s} - r\frac{h_c^2}{4}N^{\,i}_{s\theta,s} - \frac{h_c^2}{4}N^{\,o}_{\theta z} - \frac{h_c^2}{4}N^{\,i}_{\theta z} - M^{c}_{\theta2,\theta} - rM^{c}_{Q2s\theta,s} - M^{c}_{Q20z}$$
$$+2rM^{c}_{Q10z} + \frac{h_c^2}{4}n^o_s + \frac{h_c^2}{4}n^i_s = 0 \tag{42}$$

$$+\frac{h_c^3}{8}N^{\,o}_{\theta\theta,\theta} - \frac{h_c^3}{8}N^{\,i}_{\theta\theta,\theta} + r\frac{h_c^3}{8}N^{\,o}_{s\theta,s} - r\frac{h_c^3}{8}N^{\,i}_{s\theta,s} + \frac{h_c^3}{8}N^{\,o}_{\theta z} - \frac{h_c^3}{8}N^{\,i}_{\theta z} - M^{c}_{\theta3,\theta} - rM^{c}_{Q3s\theta,s} - M^{c}_{Q30z}$$
$$+3rM^{c}_{Q20z} - \frac{h_c^3}{8}n^o_s + \frac{h_c^3}{8}n^i_s = 0 \tag{43}$$

$$-N^{\,o}(w^{\,c}_0) - N^{\,i}(w^{\,c}_0) - N^{\,c}(w^{\,c}_0) + \frac{h_c}{2}N^{\,o}(w^{\,c}_1) - \frac{h_c}{2}N^{\,i}(w^{\,c}_1) - \frac{h_c^2}{4}N^{\,o}(w^{\,c}_2) - \frac{h_c^2}{4}N^{\,i}(w^{\,c}_2)$$
$$-N^{\,oT}(w^{\,c}_0) - N^{\,iT}(w^{\,c}_0) - N^{\,cT}(w^{\,c}_0) + \frac{h_c}{2}N^{\,oT}(w^{\,c}_1) - \frac{h_c}{2}N^{\,iT}(w^{\,c}_1) - \frac{h_c^2}{4}N^{\,oT}(w^{\,c}_2) - \frac{h_c^2}{4}N^{\,iT}(w^{\,c}_2)$$
$$+N^{\,o}_{\theta\theta} + N^{\,i}_{\theta\theta} - rN^{\,o}_{sz,s} - rN^{\,i}_{sz,s} - N^{\,o}_{\theta z,\theta} - N^{\,i}_{\theta z,\theta} + -R^{c}_{\theta} - rQ^{c}_{sz,s} + n^o_s + n^i_s = 0 \tag{44}$$

$$+\frac{h_c}{2}N^{\,o}(w^{\,c}_0) - \frac{h_c}{2}N^{\,i}(w^{\,c}_0) - \frac{h_c^2}{4}N^{\,o}(w^{\,c}_1) - \frac{h_c^2}{4}N^{\,i}(w^{\,c}_1) + \frac{h_c^3}{8}N^{\,o}(w^{\,c}_2) - \frac{h_c^3}{8}N^{\,i}(w^{\,c}_2)$$
$$+\frac{h_c}{2}N^{\,oT}(w^{\,c}_0) - \frac{h_c}{2}N^{\,iT}(w^{\,c}_0) - \frac{h_c^2}{4}N^{\,oT}(w^{\,c}_1) - \frac{h_c^2}{4}N^{\,iT}(w^{\,c}_1) + \frac{h_c^3}{8}N^{\,oT}(w^{\,c}_2) - \frac{h_c^3}{8}N^{\,iT}(w^{\,c}_2)$$
$$-\frac{h_c}{2}N^{\,o}_{\theta\theta} + \frac{h_c}{2}N^{\,i}_{\theta\theta} + \frac{h_c}{2}rN^{\,o}_{sz,s} - \frac{h_c}{2}rN^{\,i}_{sz,s} + \frac{h_c}{2}N^{\,o}_{\theta z,\theta} - \frac{h_c}{2}N^{\,i}_{\theta z,\theta} + M^{c}_{\theta1} + rR^{c}_{z} - rM^{c}_{Q1sz,s}$$
$$-\frac{h_c}{2}n^o_s + \frac{h_c}{2}n^i_s = 0 \tag{45}$$

$$-\frac{h_c^2}{4}N^{o}(w_0^c)-\frac{h_c^2}{4}N^{i}(w_0^c)+\frac{h_c^3}{8}N^{o}(w_1^c)-\frac{h_c^3}{8}N^{i}(w_1^c)-\frac{h_c^4}{16}N^{o}(w_2^c)-\frac{h_c^4}{16}N^{i}(w_2^c)$$
$$-\frac{h_c^2}{4}N^{oT}(w_0^c)-\frac{h_c^2}{4}N^{iT}(w_0^c)+\frac{h_c^3}{8}N^{oT}(w_1^c)-\frac{h_c^3}{8}N^{iT}(w_1^c)-\frac{h_c^4}{16}N^{oT}(w_2^c)-\frac{h_c^4}{16}N^{iT}(w_2^c)$$
$$+\frac{h_c^2}{4}N_{\theta\theta}^{o}-\frac{h_c^2}{4}N_{\theta\theta}^{i}-\frac{h_c^2}{4}rN_{sz,s}^{o}-\frac{h_c^2}{4}rN_{sz,s}^{i}-\frac{h_c^2}{4}N_{\theta z,\theta}^{o}-\frac{h_c^2}{4}N_{\theta z,\theta}^{i}+M_{\theta 2}^{c}+2rM_{z1}^{c}-rM_{Q2sz,s}^{c}$$
$$+\frac{h_c^2}{4}n_s^{o}+\frac{h_c^2}{4}n_s^{i}=0 \qquad (46)$$

where $N^{j}(w_l^c)$ is defined as follows [31]:

$$N^{j}(w_l^c)=rN_{ss,s}^{j}w_{l,s}^{c}+rN_{ss}^{j}w_{l,ss}^{c}+N_{s\theta,s}^{j}w_{l,\theta}^{c}+2N_{s\theta}^{j}w_{l,s\theta}^{c}+\frac{1}{r}N_{\theta\theta,\theta}^{j}w_{l,\theta}^{c}+\frac{1}{r}N_{\theta\theta}^{j}w_{l,\theta\theta}^{c}$$
$$;j=(o,i,c),l=(0,1,2) \qquad (47)$$

In the relations of the face sheets, the "N"s depict the in-plane stress resultants; "M"s refer to the moment resultants; and "$N_{s\theta}^{j}$ (j = o, i)"s display the out of plane shear stress resultants, respectively, which calculated as follows [1, 2]:

$$\begin{Bmatrix}N_{ss}^{j}\\N_{\theta\theta}^{j}\\N_{s\theta}^{j}\end{Bmatrix}=\begin{bmatrix}A_{11}&A_{12}&0\\A_{12}&A_{22}&0\\0&0&A_{66}\end{bmatrix}\begin{Bmatrix}\varepsilon_{ssj}^{(0)}\\\varepsilon_{\theta\theta j}^{(0)}\\\varepsilon_{s\theta j}^{(0)}\end{Bmatrix}+\begin{bmatrix}B_{11}&B_{12}&0\\B_{12}&B_{22}&0\\0&0&B_{66}\end{bmatrix}\begin{Bmatrix}\varepsilon_{ssj}^{(1)}\\\varepsilon_{\theta\theta j}^{(1)}\\\varepsilon_{s\theta j}^{(1)}\end{Bmatrix}-\begin{Bmatrix}N_{ss}^{Tj}\\N_{\theta\theta}^{Tj}\\0\end{Bmatrix} \qquad (48)$$

$$\begin{Bmatrix}M_{ss}^{j}\\M_{\theta\theta}^{j}\\M_{s\theta}^{j}\end{Bmatrix}=\begin{bmatrix}B_{11}&B_{12}&0\\B_{12}&B_{22}&0\\0&0&B_{66}\end{bmatrix}\begin{Bmatrix}\varepsilon_{ssj}^{(0)}\\\varepsilon_{\theta\theta j}^{(0)}\\\varepsilon_{s\theta j}^{(0)}\end{Bmatrix}+\begin{bmatrix}D_{11}&D_{12}&0\\D_{12}&D_{22}&0\\0&0&D_{66}\end{bmatrix}\begin{Bmatrix}\varepsilon_{ssj}^{(1)}\\\varepsilon_{\theta\theta j}^{(1)}\\\varepsilon_{s\theta j}^{(1)}\end{Bmatrix}-\begin{Bmatrix}M_{ss}^{Tj}\\M_{\theta\theta}^{Tj}\\0\end{Bmatrix} \qquad (49)$$

$$\begin{Bmatrix}N_{sz}^{j}\\N_{\theta z}^{j}\end{Bmatrix}=\frac{\pi^2}{12}\begin{bmatrix}A_{44}&0\\0&A_{55}\end{bmatrix}\begin{Bmatrix}\gamma_{szj}^{(0)}\\\gamma_{\theta zj}^{(0)}\end{Bmatrix}+\frac{\pi^2}{12}\begin{bmatrix}B_{44}&0\\0&B_{55}\end{bmatrix}\begin{Bmatrix}\gamma_{szj}^{(1)}\\\gamma_{\theta zj}^{(1)}\end{Bmatrix},\qquad j=(o,i)$$

$$M_{\theta z}^{j}=\frac{\pi^2}{12}B_{55}\gamma_{\theta zj}^{(0)}+\frac{\pi^2}{12}D_{55}\gamma_{\theta zj}^{(1)} \qquad (50)$$

Also the strain components in the Eqs. (48-50) are defined as:

$$\begin{Bmatrix}\varepsilon_{ssj}^{(0)}\\\varepsilon_{\theta\theta j}^{(0)}\\\varepsilon_{s\theta j}^{(0)}\end{Bmatrix}=\begin{Bmatrix}u_{0j,s}\\\frac{1}{r}\left(v_{0j,\theta}+w_j\right)\\\frac{1}{r}u_{0j,\theta}+v_{0j,s}\end{Bmatrix},\quad\begin{Bmatrix}\varepsilon_{ssj}^{(1)}\\\varepsilon_{\theta\theta j}^{(1)}\\\varepsilon_{s\theta j}^{(1)}\end{Bmatrix}=\begin{Bmatrix}\phi_{s,s}^{j}\\\frac{1}{r}\phi_{\theta,\theta}^{j}\\\frac{1}{r}\phi_{s,\theta}^{j}+\phi_{\theta,s}^{j}\end{Bmatrix} \qquad (51)$$

$$\begin{Bmatrix}\gamma_{szj}^{(0)}\\\gamma_{\theta zj}^{(0)}\end{Bmatrix}=\begin{Bmatrix}w_{j,s}+\varphi_s^j\\\frac{1}{r}\left(w_{j,\theta}-v_{0j}\right)+\varphi_\theta^j\end{Bmatrix},\quad\begin{Bmatrix}\gamma_{szj}^{(1)}\\\gamma_{\theta zj}^{(1)}\end{Bmatrix}=\begin{Bmatrix}0\\\frac{-\varphi_\theta^j}{r}\end{Bmatrix} \qquad (52)$$

It should be noted that $\frac{\pi^2}{12}$ is the shear correction factor in FSDT. Also, N_{ss}^{Tj}, $N_{\theta\theta}^{Tj}$, M_{ss}^{Tj} and $M_{\theta\theta}^{Tj}$ are the thermal stress resultants. "A" is the stretching stiffness; "B" is the bending-stretching stiffness; and "D" is the bending stiffness; which are constant coefficients and express as:

$$N_{ss}^{Tj}=N_{\theta\theta}^{Tj}=\int_{-\frac{h_j}{2}}^{\frac{h_j}{2}}\frac{E_j(z_j,T_j)}{1-\upsilon_j(z_j,T_j)}.\alpha_j(z_j,T_j).\Delta T_j.dz_j\quad,\qquad j=(o,i) \qquad (53)$$

$$M_{ss}^{Tj} = M_{\theta\theta}^{Tj} = \int_{-\frac{h_j}{2}}^{\frac{h_j}{2}} \frac{z_j.E_j(z_j,T_j)}{1-\upsilon_j(z_j,T_j)}.\alpha_j(z_j,T_j).\Delta T_j dz_j \quad , \quad j=(o,i) \tag{54}$$

$$\begin{Bmatrix} A_{11}^j \\ B_{11}^j \\ D_{11}^j \end{Bmatrix} = \begin{Bmatrix} A_{22}^j \\ B_{22}^j \\ D_{22}^j \end{Bmatrix} = \int_{-\frac{h_j}{2}}^{\frac{h_j}{2}} \left[\frac{E_j(z_j,T_j)}{1-\left(\upsilon_j(z_j,T_j)\right)^2} \right] \begin{Bmatrix} 1 \\ z_j \\ z_j^{\,2} \end{Bmatrix} dz_j \tag{55}$$

$$\begin{Bmatrix} A_{12}^j \\ B_{12}^j \\ D_{12}^j \end{Bmatrix} = \int_{-\frac{h_j}{2}}^{\frac{h_j}{2}} \left[\frac{\upsilon_j(z_j,T_j)\times E_j(z_j,T_j)}{1-\left(\upsilon_j(z_j,T_j)\right)^2} \right] \begin{Bmatrix} 1 \\ z_j \\ z_j^{\,2} \end{Bmatrix} dz_j \tag{56}$$

$$\begin{Bmatrix} A_{66}^j \\ B_{66}^j \\ D_{66}^j \end{Bmatrix} = \int_{-\frac{h_j}{2}}^{\frac{h_j}{2}} \left[\frac{E_j(z_j,T_j)}{2\left(1+\upsilon_j(z_j,T_j)\right)} \right] \begin{Bmatrix} 1 \\ z_j \\ z_j^{\,2} \end{Bmatrix} dz_j \tag{57}$$

where $E_j(z_j,T_j)$, $\upsilon_j(z_j,T_j)$ and $\alpha_j(z_j,T_j)$, $j=(o,i)$ are the modulus of elasticity, Poisson's ratio and the thermal expansion coefficient of the FG face sheets, respectively, and introduced by power-law function of FGMs. "o" and "i" refer to the outer and inner face sheet layers, respectively. And also, twenty three stress resultants of the core are defined as:

$$\left\{Q_{sz}^c, M_{Q1sz}^c, M_{Q2sz}^c, M_{Q3sz}^c\right\} = \int_{-\frac{h_c}{2}}^{\frac{h_c}{2}} \left(1, z_c, {z_c}^2, {z_c}^3\right) \tau_{sz}^c dz_c \tag{58}$$

$$\left\{Q_{\theta z}^c, M_{Q1\theta z}^c, M_{Q2\theta z}^c, M_{Q3\theta z}^c\right\} = \int_{-\frac{h_c}{2}}^{\frac{h_c}{2}} \left(1, z_c, {z_c}^2, {z_c}^3\right) \tau_{\theta z}^c dz_c \tag{59}$$

$$\left\{R_z^c, M_{z1}^c, M_{z2}^c\right\} = \int_{-\frac{h_c}{2}}^{\frac{h_c}{2}} \left(1, z_c, {z_c}^2\right) \sigma_{zz}^c dz_c \tag{60}$$

$$\left\{Q_{s\theta}^c, M_{Q1s\theta}^c, M_{Q2s\theta}^c, M_{Q3s\theta}^c\right\} = \int_{-\frac{h_c}{2}}^{\frac{h_c}{2}} \left(1, z_c, {z_c}^2, {z_c}^3\right) \tau_{s\theta}^c dz_c \tag{61}$$

$$\left\{R_s^c, M_{s1}^c, M_{s2}^c, M_{s3}^c\right\} = \int_{-\frac{h_c}{2}}^{\frac{h_c}{2}} \left(1, z_c, {z_c}^2, {z_c}^3\right) \sigma_{ss}^c dz_c \tag{62}$$

$$\left\{R_\theta^c, M_{\theta 1}^c, M_{\theta 2}^c, M_{\theta 3}^c\right\} = \int_{-\frac{h_c}{2}}^{\frac{h_c}{2}} \left(1, z_c, {z_c}^2, {z_c}^3\right) \sigma_{\theta\theta}^c dz_c \tag{63}$$

Finally, by substituting the high order stress resultants in terms of the kinematic relations, the equations are derived in terms of the nine unknowns.

Eq. (47) can be rewritten as [31]:

$$N(w_l^c) = r\hat{N}_{ss,s}^{\,j} w_{l,s}^c + r\hat{N}_{ss}^{\,j} w_{l,ss}^c + \hat{N}_{s\theta,s}^{\,j} w_{l,\theta}^c + 2\hat{N}_{s\theta}^{\,j} w_{l,s\theta}^c + \tfrac{1}{r}\hat{N}_{\theta\theta,\theta}^{\,j} w_{l,\theta}^c + \tfrac{1}{r}\hat{N}_{\theta\theta}^{\,j} w_{l,\theta\theta}^c$$
$$; j=(o,i,c), l=(0,1,2) \tag{64}$$

where $\hat{N}^{j}_{ss}$, $\hat{N}^{j}_{\theta\theta}$ and $\hat{N}^{j}_{s\theta}$ are the external in-plane loads exerted to the top and bottom face sheets and the core. Therefore

$$N(w_l^c) = \hat{N}^{j}_{ss} w^{c}_{l,ss} + 2\hat{N}^{j}_{s\theta} w^{c}_{l,s\theta} + \hat{N}^{j}_{\theta\theta} w^{c}_{l,\theta\theta} \qquad (65)$$

The axial in-plane compressive load $\hat{N}^{j}_{ss}$s, , are the parts of total external load, $\hat{N}_0$, as follows:

$$N^{o}_{ss} + N^{i}_{ss} + N^{c}_{ss} = -N_0 \qquad (66)$$

In this analysis, uniform state of strain for the face sheets and the core is assumed. At edges "s=0" or "s=L" and with a little simplification the equilibrium equations can be defined as:

$$\frac{N^{o}_{ss}}{h_o \bar{E}_o} = \frac{N^{i}_{ss}}{h_i \bar{E}_i} = \frac{N^{c}_{ss}}{h_c \bar{E}_c} \qquad (67)$$

where $\bar{E}_j$ is the equilibrium elasticity modulus of the layers that are defined as:

$$\bar{E}_j = \frac{\int_{-h_j/2}^{h_j/2} E_j(z_j)\,dz_j}{h_j}; \; j = (o,i,c) \qquad (68)$$

Hence, by using of Eq. (67) and (68), the external in-plane loads exerted to the face sheets and the core along the "s" direction can be obtained as:

$$\begin{Bmatrix} N^{o}_{ss} \\ N^{i}_{ss} \\ N^{c}_{ss} \end{Bmatrix} = \frac{-N_0}{h_o \bar{E}_o + h_i \bar{E}_i + h_c \bar{E}_c} \begin{Bmatrix} h_o \bar{E}_o \\ h_i \bar{E}_i \\ h_c \bar{E}_c \end{Bmatrix} \qquad (69)$$

3. VERIFICATION AND NUMERICL RESULTS

A Galerkin procedure is applied to solve the governing equations of FG sandwich cylindrical shells, with trigonometric shape functions, which satisfy the boundary condition. And the shape functions of the clamped-free boundary condition can be expressed as [32]:

$$u_{ck} = C_{uk} \frac{\lambda_m}{L}\left(\sinh\left(\frac{\lambda_m s}{L}\right) + \sin\left(\frac{\lambda_m s}{L}\right) - \gamma_m\left(\cos h\left(\frac{\lambda_m s}{L}\right) - \cos\left(\frac{\lambda_m s}{L}\right)\right)\right)\cos(n\theta) \;, k = (0,1,2,3) \qquad (70)$$

$$v_{ck} = C_{vk}\left(\cosh\left(\frac{\lambda_m s}{L}\right) - \cos\left(\frac{\lambda_m s}{L}\right) - \gamma_m\left(\sin h\left(\frac{\lambda_m s}{L}\right) - \sin\left(\frac{\lambda_m s}{L}\right)\right)\right)\sin(n\theta) \qquad (71)$$

$$w_{ck} = C_{wk}\left(\cosh\left(\frac{\lambda_m s}{L}\right) - \cos\left(\frac{\lambda_m s}{L}\right) - \gamma_m\left(\sin h\left(\frac{\lambda_m s}{L}\right) - \sin\left(\frac{\lambda_m s}{L}\right)\right)\right)\cos(n\theta) \qquad (72)$$

$$\phi^{j}_{s} = C_{\phi sj} \frac{\lambda_m}{L}\left(\sinh\left(\frac{\lambda_m s}{L}\right) + \sin\left(\frac{\lambda_m s}{L}\right) - \gamma_m\left(\cos h\left(\frac{\lambda_m s}{L}\right) - \cos\left(\frac{\lambda_m s}{L}\right)\right)\right)\cos(n\theta), \; j = (o,i) \qquad (73)$$

$$\phi^{j}_{\theta} = C_{\phi\theta j}\left(\cosh\left(\frac{\lambda_m s}{L}\right) - \cos\left(\frac{\lambda_m s}{L}\right) - \gamma_m\left(\sin h\left(\frac{\lambda_m s}{L}\right) - \sin\left(\frac{\lambda_m s}{L}\right)\right)\right)\sin(n\theta) \qquad (74)$$

Which γ_m and λ_m should satisfy the conditions as follow:

$$\cos\lambda_m . \cosh\lambda_m = -1; \;\; \lambda_m = 1.875, 4.694, \ldots \qquad (75)$$

$$\gamma_m = \frac{\sinh\lambda_m - \sin\lambda_m}{\cosh\lambda_m - \cos\lambda_m} \quad m = (1,2,3,\ldots) \qquad (76)$$

where "$a_m = m\pi / L$"; "m" is the wave number and "$C_{uk}, C_{wk}, C_{\phi j}$" are the nine unknown constants of the shape functions. These fifteen equations can be displayed with a 15×15 matrix as follows:

$$(k_m - N_0 \times G_m) C_m = 0 \qquad (77)$$

Cm is the eigen vector which contains fifteen unknown constants; “G” is the geometric and “K” is the stiffness matrices.

To verify the approach of this study, present results are compared with the results of the literatures [33], [34], [35] and [36]. Consider a simply supported metallic isotropic cylindrical shell with structural parameters such as h = 0.001m, L=2R, E=200 GPa and ν=0.3. These comparisons are shown in Table 1.

Table 1. Buckling pressure for cylindrical isotropic panel

L/R	Present study	[33]	[34]	[35]	[36]
0.5	2765.4	2768.1	2766.2	2761.4	2767.4
1	1272.9	1272.0	1269.6	1272.6	1273.1
2	611.7	611.6	607.3	611.7	611.7
3	408.5	411.9	407.2	402.6	412.6

Now, consider a FG sandwich cylindrical shell which is assumed to be made from a mixture of Silicon nitride as ceramic phases and Stainless steel as metal phases. The temperature-dependent properties of constituent materials which is introduced by Eq. (1) are available in reference [37]. In general, “ht-hc-hb” sandwich shell is a structure with the indices of top face sheet thickness, core thickness and bottom face sheet thickness equal to “ht”, “hc” and “hb”, respectively. Therefore, in 1-8-1 sandwich, the thickness of the core is eight times of each face sheet thickness. For simplicity, the non-dimensional critical load parameter is defined as follows:

$$N_{cr} = \frac{N_0}{10^9} \qquad (78)$$

The material properties of structures are affected in high temperature conditions. Based on Eq. (1), increasing the temperature reduces the material properties of metal and ceramic. As a result, the strength of the panels reduces, which is an important reason in decreasing the critical load in high temperature conditions. Figure 2 shows the critical parameter variation versus the temperature for 1-8-1 FG sandwich cylindrical shell with clamped-free (C-F) boundary condition. Geometrical parameters are “h=0.02m, L/R=2, m=1, R=50h”. By increasing the temperature, the critical load parameters decrease. As shown in Figure 2, when N=0, the FG layers are made of full ceramic, as a result, the stability and resistant against the high temperature conditions are more than the other values of “N”, so critical load parameters are higher than others. By increasing the power law index, “N”, the amount of the ceramic reduces in the structure which causes the young modulus of the FGM and the stability of the structures decrease. When N=2, the amount of the ceramic is decreased in the FG layers, so, in the high temperature the stability of the structure is lower. Also, when “N=0”, by increasing the temperature, the critical load parameter decreases 47.40%, for “N=1” and “N=2” it decreases 50.31%, and 51.24%, respectively.

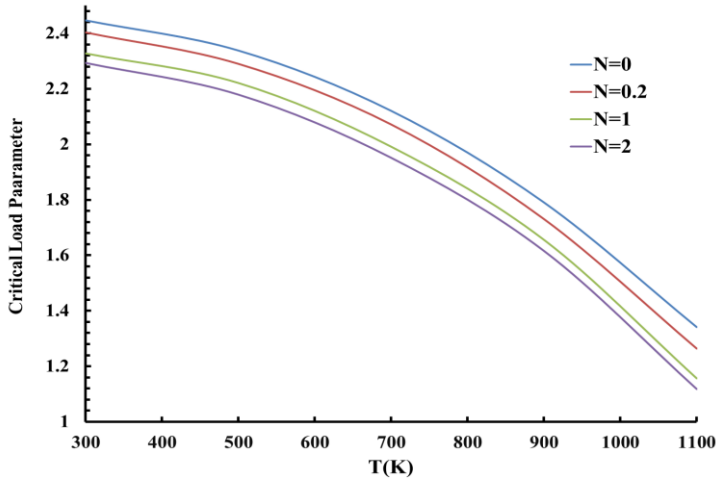

Fig. 2. Critical load variation versus temperature in FG sandwich cylindrical shell

Figure 3 shows the effect of radius to thickness ratio (R/h) on the critical load parameter for 1-8-1 FG sandwich cylindrical shell in the clamped-free (C-F) boundary condition. Geometrical parameters are “h = 0.02m, T=300K, m=1, L=2R”. For R/h<40, when ratios are increased in a constant “N”, the critical load

parameter decreasesd, but for R/h>40 the critical loads increase. Based on the Fig. 3, by increasing of this ratio, the stability of the structure reduces and it is important to consider that long length is not proper for the FG sandwich cylinder. Also, it is obvious that, by increasing the power law index, “N”, the critical load parameters decrease, but in this case effect of variation of the radius is dominant parameter and its variation has an impressive effect on the stability. For example, for "R/h=20", by increasing “N”, the critical load parameter decrease 11.29%, but for “N=0”, by increasing this ratio, first the critical load parameter decreases 88.62%, then after the ratio R/h>40 increseases 44.16%.

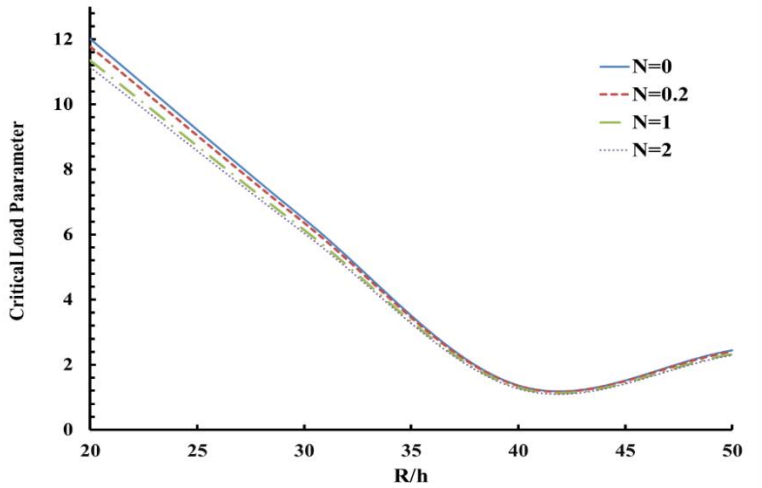

Fig. 3. Critical load variation versus R/h ratio in sandwich cylindrical shell.

Figure 4 shows the variation of the core to face sheet thickness ratio, “hc/ho”, on the critical load parameter in various power law indices and in a constant total thickness. Geometrical parameters are “h=0.02m, T=300K, m=1, R/h=50, L=2R”. When “hc/ho=0.5”, it means the face sheets thicknesses are two times of the core thickness, so it shows the results of the 2-1-2 sandwich. And, when “hc/ht=8”, it shows results of the 1-8-1 sandwich. By increasing the ratio in a constant thickness and N, the critical load parameters increase. By increasing the power law index in a constant thickness, ceramic quantity of FG layer decreases, so, for all values of “hc/ho”, the critical load parameters decrease. In “hc/ho=0.5”, the critical load parameter decreases 60.11%, when “N” is increased, and in “hc/ho=8”, the critical load parameter decreases 6.27% when “N” is increased. Also, for “N=0”, by increasing this ratio, the critical load increases 52.74%, but for "N=2", it increases 79.89%.

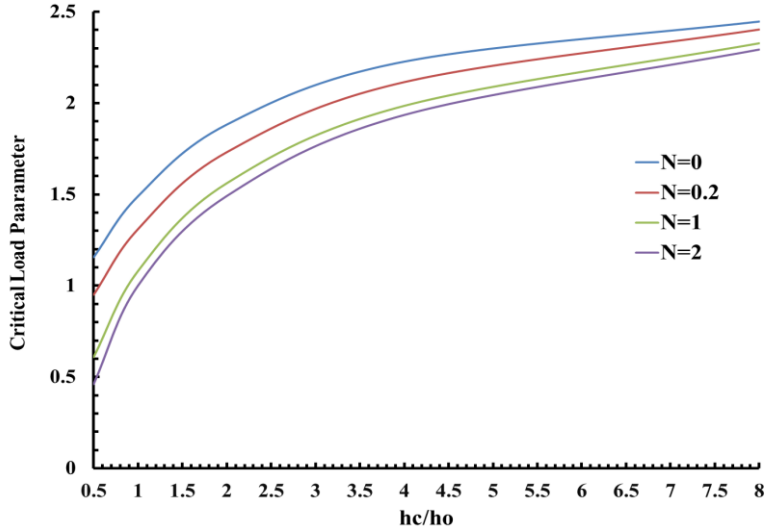

Fig. 4. Critical load variation versus “hc/ho” ratio in FG sandwich cylindrical shell

Effect of the variation of the length to radius of the sandwiches, “L/R”, on the critical load parameter in various power law indices for FG sandwich shell is depicted in Figure 5. Geometrical parameters are “T=300K, m=1, R/h=50”. It is obvious that by increasing the Ratios in a constant “N”, the critical load parameter decreases. The slope of decreasing the critical load in the value of lower than L/R<1 is sever, but in the higher values, the slope of decreasing is very low. It means after a certain value, increasing the L/R has a little effect on the critical load. For example, when “N=0”, by increasing the “L/R”, first the critical load decrease 57.30%, and after the L/R>1, it decreases 3.77%.

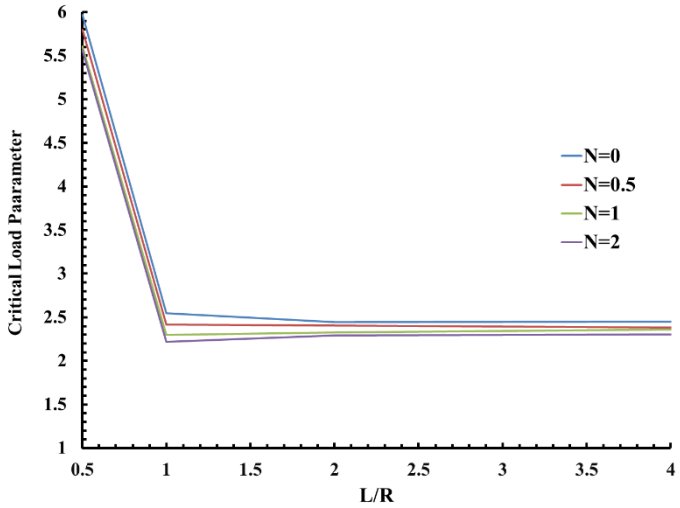

Fig. 5. Critical load variation versus thickness in different types of sandwich cylindrical shell

In order to clearly understand the porosity influence, Fig. 6 and Fig. 7 show the effect of even and uneven porosity distributions on the critical load parameters of the FG sandwich cylindrical shell, respectively. As shown in Fig. 6, by increasing the porosity volume fraction, first the critical load parameter increases, but after a certain value of N, the behavior of the critical load changes and it starts to decrease in higher value of N. In even distributions, porosities occur all over the cross-section of FG layer. While, in uneven distribution, porosities are available at middle zone of cross section. For the even case and “N=0”, by increasing the volume fraction of the porosity, the critical load increases 0.69%, but for N=2, it decrease 0.056%. On the other hand, based on the Fig.7, by increasing the porosity volume fraction, the critical load parameter increases for all values of N. In the uneven case in “N=0”, by increasing the volume fraction of the porosity, the critical load increaases 1.79%, and In N=2, it increase 1.51%.

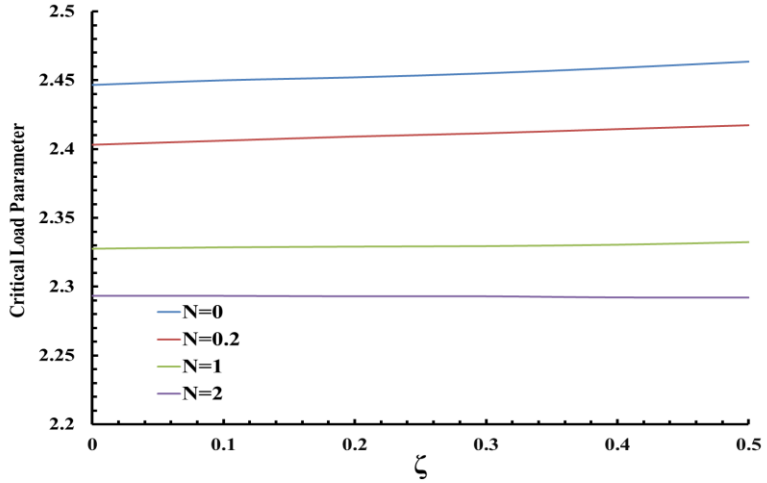

Fig. 6. Critical load variation versus even porosity in FG sandwich cylindrical shell

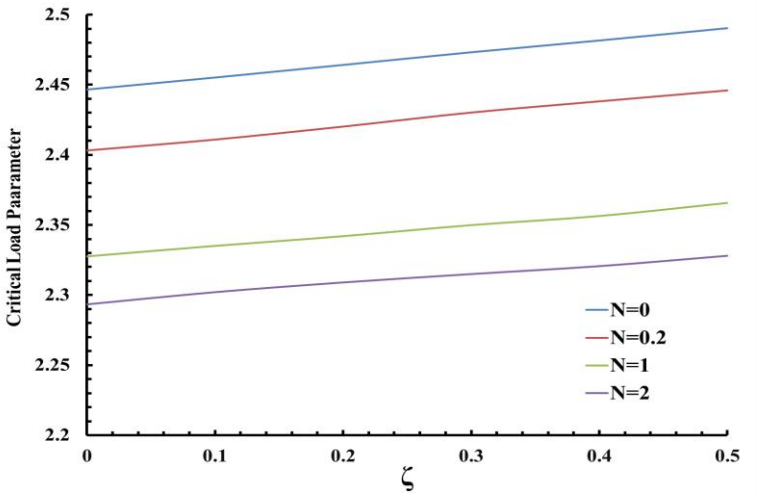

Fig. 7. Critical load variation versus uneven porosity in FG sandwich cylindrical shell

4. CONCUSION

By applying a modified high-order sandwich shell theory and considering the high-order stress resultants and thermal stress resultants, in plane stresses and thermal stresses, and nonlinear strains in face-sheets and core, buckling behavior of porous FG cylidrical sandwich shells which were temperature dependent, was investigated in this paper. The displacement fields of the face-sheets and the core were considered based on the first order shear deformation theory and the polynomial distributions, respectively. A power law distribution which modified by considering even and uneven porosity distributions was used to model the material properties of the FG layers. The FG layers were location dependent too. The governing equations were obtained by minimum potential energy principal and solved by using Galerkin method for clamped-free boundary condition. Also, a method was applied to reduce the number of the equations. Effects of temperature, thickness, length, radius and porosities distributions on the critical load were discussed. The following conclusion can be drawn:

- By increasing the temperature, the critical load parameters decrease.
- By increasing the power law index, the critical load parameters decrease.
- By increasing the radius to thickness ratio, first the critical load parameter decreases and then increase slowly.
- By increasing the the core to face-sheet thickness ratio, the critical load parameters increase.
- By increasing the length to radius ratio in a constant N, the critical load parameters decrease.
- By increasing the porosity volume fraction in even distribution, first the critical load parmeter increases, but after a certain value of N, it start to decrease.
- In uneven distributions, the critical load parameters increase.

REFERENCES

[1] Rahmani M, Mohammadi Y, Kakavand F. (2019). Vibration analysis of sandwich truncated conical shells with porous FG face sheets in various thermal surroundings. *Steel and Composite Structures*, vol. 32, no. 2, p. 239-252.

[2] Rahmani M, Mohammadi Y, Kakavand F, Raeisifard H. (2020). Vibration analysis of different types of porous FG conical sandwich shells in various thermal surroundings. *Journal of Applied and Computational Mechanics*, vol. 6, no. 3, p. 416-432.

[3] Frostig Y, Baruch M, Vilnay O, Sheinman I. (1992). High-order theory for sandwich-beam

behavior with transversely flexible core. *Journal of Engineering Mechanics*, vol. 118, no. 5, p. 1026-1043.

[4] Lopatin A, Morozov E. (2015). Buckling of the composite sandwich cylindrical shell with clamped ends under uniform external pressure. *Composite Structures*, vol. 122, p. 209-216.

[5] Ghahfarokhi DS, Rahimi G. (2018). An analytical approach for global buckling of composite sandwich cylindrical shells with lattice cores. *International Journal of Solids and Structures*, vol. 146, p. 69-79.

[6] Hieu PT, Tung HV. (2021). Nonlinear buckling behavior of functionally graded material sandwich cylindrical shells with tangentially restrained edges subjected to external pressure and thermal loadings. *Journal of Sandwich Structures & Materials*, vol. 23, no. 6, p. 2000-2027.

[7] Eslami MR, Eslami J, Jacobs M. (2018). *Buckling and postbuckling of beams, plates, and shells*, Springer.

[8] Nam VH, Phuong NT, Trung NT. (2019). Nonlinear buckling and postbuckling of sandwich FGM cylindrical shells reinforced by spiral stiffeners under torsion loads in thermal environment. *Acta Mechanica*, vol. 230, no. 9, p. 3183-3204.

[9] Fallah F, Taati E. (2019). On the nonlinear bending and post-buckling behavior of laminated sandwich cylindrical shells with FG or isogrid lattice cores. *Acta Mechanica*, vol. 230, no. 6, p. 2145-2169.

[10] Balbin IU, Bisagni C. (2021). Buckling of sandwich cylindrical shells with shear deformable core through nondimensional parameters. *Thin-Walled Structures*, vol. 161, p. 107393.

[11] Chan DQ, Van Hoan P, Trung NT, Hoa LK, Huan DT. (2021). Nonlinear buckling and post-buckling of imperfect FG porous sandwich cylindrical panels subjected to axial loading under various boundary conditions. *Acta Mechanica*, vol. 232, no. 3, p. 1163-1179.

[12] Tho Hung V, Thuy Dong D, Thi Phuong N, et al. (2020). Nonlinear buckling behavior of spiral corrugated sandwich FGM cylindrical shells surrounded by an elastic medium. *Materials*, vol. 13, no. 8, p. 1984.

[13] Semenyuk N, Trach V, Zhukova N. (2019). Stability and initial post-buckling behavior of orthotropic cylindrical sandwich shells with unidirectional elastic filler. *International Applied Mechanics*, vol. 55, no. 6, p. 636-647.

[14] MalekzadehFard K, Gholami M, Reshadi F, Livani M. (2017). Free vibration and buckling analyses of cylindrical sandwich panel with magneto rheological fluid layer. *Journal of Sandwich Structures & Materials*, vol. 19, no. 4, p. 397-423.

[15] Shatov, A. V., A. E. Burov, and A. V. Lopatin. (2020). Buckling of composite sandwich cylindrical shell with lattice anisogrid core under hydrostatic pressure. *Journal of Physics: Conference Series*, vol. 1546, no. 1, p. 012139. IOP Publishing,.

[16] Nam VH, Trung N-T. (2019). Buckling and postbuckling of porous cylindrical shells with functionally graded composite coating under torsion in thermal environment. *Thin-Walled Structures*, vol. 144, p. 106253.

[17] Phuong NT, Nam VH, Trung NT, Duc VM, Phong PV. (2019). Nonlinear stability of sandwich functionally graded cylindrical shells with stiffeners under axial compression in thermal environment. *International Journal of Structural Stability and Dynamics*, vol. 19, no. 07, p. 1950073.

[18] Han Q, Wang Z, Nash DH, Liu P. (2017). Thermal buckling analysis of cylindrical shell with functionally graded material coating. *Composite Structures*, vol. 181, p. 171-182.

[19] Evkin AY. (2019). Local buckling of cylindrical shells. Pogorelov's geometrical method. *Problems of Nonlinear Mechanics and Physics of Materials: Springer*, p. 369-391.

[20] Trabelsi S, Frikha A, Zghal S, Dammak F. (2019). A modified FSDT-based four nodes finite shell element for thermal buckling analysis of functionally graded plates and cylindrical shells. *Engineering Structures*, vol. 178, p. 444-459.

[21] Mehralian F, Beni YT. (2016). Size-dependent torsional buckling analysis of functionally graded cylindrical shell. *Composites Part B: Engineering*, vol. 94, p. 11-25.

[22] Fan H. (2019). Critical buckling load prediction of axially compressed cylindrical shell based on non-destructive probing method. *Thin-Walled Structures*, vol. 139, p. 91-104.

[23] Sofiyev A, Hui D. (2019). On the vibration and stability of FGM cylindrical shells under external pressures with mixed boundary conditions by using FOSDT. *Thin-Walled Structures*, vol. 134, p. 419-427.

[24] Gao K, Gao W, Wu D, Song C. (2018). Nonlinear dynamic stability of the orthotropic functionally graded cylindrical shell surrounded by Winkler-Pasternak elastic foundation subjected to a linearly increasing load. *Journal of Sound and Vibration*, vol. 415, p. 147-168.
[25] Sheng G, Wang X. (2018). The dynamic stability and nonlinear vibration analysis of stiffened functionally graded cylindrical shells. *Applied Mathematical Modelling*, vol. 56, p. 389-403.
[26] Sofiyev AH, Hui D, Valiyev A, et al. (2016). Effects of shear stresses and rotary inertia on the stability and vibration of sandwich cylindrical shells with FGM core surrounded by elastic medium. *Mechanics Based Design of Structures and Machines*, vol. 44, no. 4, p. 384-404.
[27] Asadi H, Akbarzadeh A, Chen Z, Aghdam M. (2015). Enhanced thermal stability of functionally graded sandwich cylindrical shells by shape memory alloys. *Smart Materials and Structures*, vol. 24, no. 4, p. 045022.
[28] Rahmani M, Mohammadi Y, Kakavand F. (2020). Buckling analysis of different types of porous FG conical sandwich shells in various thermal surroundings. *Journal of the Brazilian Society of Mechanical Sciences and Engineerin*,vol. 42, no. 4, p. 1-16.
[29] Rahmani M, Mohammadi Y, Kakavand F, Raeisifard H. (2019). Buckling behavior analysis of truncated conical sandwich panel with porous FG core in different thermal conditions. *Amirkabir Journal of Mechanical Engineering*, vol. 52, no. 10, p. 141-150.
[30] Rahmani M, Dehghanpour S. (2021). Temperature-Dependent Vibration of Various Types of Sandwich Beams with Porous FGM Layers. *International Journal of Structural Stability and Dynamics*, vol. 21, no. 2, p. 2150016.
[31] Kheirikhah M, Khalili S, Fard KM. (2012). Biaxial buckling analysis of soft-core composite sandwich plates using improved high-order theory. *European Journal of Mechanics-A/Solids*, vol. 31, no. 1, p. 54-66.
[32] Rahmani M, Mohammadi Y. (2021). Vibration of two types of porous FG sandwich conical shell with different boundary conditions. *Structural Engineering and Mechanics*, vol. 79, no. 4, p. 401-413.
[33] Fard KM, Livani M. (2015). The buckling of truncated conical sandwich panels under axial compression and external pressure. *Proceedings of the Institution of Mechanical Engineers, Part C: Journal of Mechanical Engineering Science*, vol. 229, no. 11, p. 1965-1978.
[34] Vodenitcharova T, Ansourian P. (1996). Buckling of circular cylindrical shells subject to uniform lateral pressure. *Engineering Structures*, vol. 18, no. 8, p. 604-614.
[35] Shen H-S. (2003). Postbuckling analysis of pressure-loaded functionally graded cylindrical shells in thermal environments. *Engineering Structures*, vol. 25, no. 4, p. 487-497.
[36] Khazaeinejad P, Najafizadeh M. (2010). Mechanical buckling of cylindrical shells with varying material properties. *Proceedings of the Institution of Mechanical Engineers, Part C: Journal of Mechanical Engineering Science*, vol. 224, no. 8, p. 1551-1557.
[37] 37. Reddy JN. (2003). *Mechanics of laminated composite plates and shells: theory and analysis*, CRC press.